

Genomes & Developmental Control

# Computational identification of microRNA targets

Nikolaus Rajewsky<sup>a,\*</sup> and Nicholas D. Socci<sup>b,c</sup>

<sup>a</sup>Department of Biology, New York University, New York, NY 10003-6688, USA

<sup>b</sup>Department of Pathology, and Seaver Foundation for Bioinformatics, Albert Einstein College of Medicine, Bronx, NY 10461, USA

<sup>c</sup>Computational Biology Center, Memorial Sloan-Kettering Cancer Center, New York, NY 10021, USA

Received for publication 12 October 2003, revised 22 November 2003, accepted 1 December 2003

## Abstract

Recent experiments have shown that the genomes of organisms such as worm, fly, human, and mouse encode hundreds of microRNA genes. Many of these microRNAs are thought to regulate the translational expression of other genes by binding to partially complementary sites in messenger RNAs. Phenotypic and expression analysis suggests an important role of microRNAs during development. Therefore, it is of fundamental importance to identify microRNA targets. However, no experimental or computational high-throughput method for target site identification in animals has been published yet. Our main result is a new computational method that is designed to identify microRNA target sites. This method recovers with high specificity known microRNA target sites that have previously been defined experimentally. Based on these results, we present a simple model for the mechanism of microRNA target site recognition. Our model incorporates both kinetic and thermodynamic components of target recognition. When we applied our method to a set of 74 *Drosophila melanogaster* microRNAs, searching 3' UTR sequences of a predefined set of fly mRNAs for target sites which were evolutionary conserved between *D. melanogaster* and *Drosophila pseudoobscura*, we found that many key developmental body patterning genes such as *hairy* and *fushi-tarazu* are likely to be translationally regulated by microRNAs.

© 2003 Elsevier Inc. All rights reserved.

**Keywords:** MicroRNA; miRNA; Computational; Translational regulation; cis-regulatory sites; Target sites; Development; Body patterning

## Introduction

MicroRNA (miRNA) genes are a new and large class of genes that do not encode proteins. They produce roughly 22-nucleotide-long transcripts that in many cases are thought to function as antisense regulators of other mRNAs (Ambros, 2001). By now, hundreds of miRNAs in human, mouse, worm, and fly have been identified using molecular and computational approaches (Ambros et al., 2003; Aravin et al., 2003; Lagos-Quintana et al., 2001; Lai et al., 2003; Lau et al., 2001; Lee and Ambros, 2001; Lim et al., 2003a,b). So far, however, the biological function of miRNAs has been elucidated in only a few examples (*lin-4* and *let-7* in *Caenorhabditis elegans*, *bantam* and *mir-14* in fly, and *microRNA-23* in human). *lin-4* and *let-7* are involved in the timing of developmental

processes (heterochronic genes), *bantam* has been shown to affect cell proliferation and death (Brennecke et al., 2003), and *mir-14* regulates the expression of the cell death pathway and fat metabolism (Xu et al., 2003). These results suggest a broad range of possible functions for miRNAs. The overall importance of miRNAs for development has been further established by the notion that many miRNAs appear to have temporal or tissue-specific patterns of gene expression (Ambros et al., 2003; Aravin et al., 2003; Houbaviv et al., 2003; Lagos-Quintana et al., 2002; Lau et al., 2001; Lim et al., 2003b).

In most known cases in animals, miRNAs regulate the translational expression of genes. miRNAs are thought to bind partially complementary sites in 3' untranslated regions of mature target mRNA in the cytoplasm and, by unknown mechanisms, to modulate (repress) translation of the target mRNA (for reviews, see Ambros, 2001, 2003; Banerjee and Slack, 2002; Carrington and Ambros, 2003; Moss, 2002; Moss and Poethig, 2002). To understand the biological function of miRNAs, it is necessary to identify their targets. No high-throughput experimental techniques for target site identification have been reported yet. Computational

\* Corresponding author. Department of Biology, New York University, 1009 Main Building, 100 Washington Square East, New York, NY 10003-6688. Fax: +1-212-995-4015.

E-mail address: [nikolaus.rajewsky@nyu.edu](mailto:nikolaus.rajewsky@nyu.edu) (N. Rajewsky).

approaches have been successful in plants, where known target sites tend to be almost perfectly complementary to miRNAs (Rhoades et al., 2002) and where miRNAs are thought to promote degradation of the target mRNA (for a review, see Carrington and Ambros, 2003). In animals, however, the miRNA/mRNA base pairing appears to be less than perfect, which has greatly hindered computational approaches for target site identification.

Here, we report on a first computational method for miRNA target site identification in animals. We set out by compiling a set of experimentally reasonably well-established target sites from the literature. Our dataset comprised 25 target sites (training set) for *lin-4* and *let-7* in *C. elegans*. We then found an algorithm that recovers most of these sites with high specificity when compared to random sites. A simple and intuitive model for kinetic and thermodynamic aspects of target site recognition is consistent with this method.

We applied our algorithm to a previously cloned and sequenced set of miRNAs in fly (Aravin et al., 2003; Lai et al., 2003). We find highly scoring, conserved putative target sites in several key developmental body-patterning transcription factors such as *fushi-tarazu* and *hairy*. Further computational analysis with existing tools (Rajewsky et al., 2002) suggests that some of the miRNA genes such as *mir-263b* may have enhancers with binding sites for subsets of the body-patterning transcription factors.

## Materials and methods

### *A set of 25 experimentally defined miRNA binding sites (Training set)*

The training set consisted of 25 experimentally defined target sites (see Banerjee and Slack, 2002; Lin et al., 2003 and references therein) of the *C. elegans* miRNAs *lin-4* and *let-7*. We padded these sites with the corresponding genomic sequences such that each site had a length of 30 nucleotides. Our 25 pairs are as follows: three pairs *lin-14/let-7*; seven pairs *lin-14/lin-4*, *lin-28/let-7*, *lin-28/lin-4*; two pairs of *lin-41/let-7*, *lin-41/lin-4*; two pairs *hbl/lin-4*; and eight pairs of *hbl/let-7*.

### *Random sequences*

Random sequences were produced by site-independent sampling of specified ACGU background frequencies. We used background frequencies of ( $p_A = 0.34$ ,  $p_C = 0.19$ ,  $p_G = 0.18$ ,  $p_U = 0.29$ ). These frequencies are consistent with the sequence composition of the *C. elegans* 3' UTRs of the target genes in our training set, and match the base frequencies of 3' UTRs from the set of all known full-length *Drosophila melanogaster* cDNAs. We checked that we obtained very similar base frequencies when mapping the 3' UTRs to *Drosophila pseudoobscura* (see below).

### *Using MFOLD to predict the secondary structure and free energy of RNA/RNA duplexes*

The second step of our algorithm involves in silico hybridization of the mature miRNA to RNA using the MFOLD RNA folding program (Zuker, 2003). Note that just joining the two RNA sequences with some linker residues and then running MFOLD would produce unreliable results because the linker residues would be treated like an interior loop and would introduce incorrect contributions to the free energy. However, the new MFOLD software allowed us to overcome this problem (Zuker, 2003). First, the two RNA sequences were joined together with an artificial linking segment of non-nucleotide elements (represented by the symbol L). For example, if one sequence was 5' -ACGTACGT-3' and the other was 5' -GCATGCAT-3', the resulting artificial single sequence is 5' -ACGTACGTLGGCATGCAT-3'. The remaining step is to prevent any base pairing within the original two sequences. Following Zuker (2003), this was accomplished by passing a special configuration file to the MFOLD program which prohibits pairing within a given range of bases. The MFOLD program was run with a temperature setting of 20°C and default parameters otherwise.

### *A set of 74 Drosophila miRNA genes*

The miRNAs used in this study came from two sources. A set of 62 miRNAs was found experimentally via the cloning of small RNAs in *D. melanogaster* (Aravin et al., 2003) that were kindly provided to us by Tom Tuschl before publication. A second set came from a computational study of Lai et al. (2003). This set was identified by searching both *melanogaster* and *pseudoobscura* genomic sequences for short conserved sequences with an extended stem-loop structure and a given pattern of divergence between the two species. We BLASTed the second set against the first and found 12 non-redundant miRNAs (*miR-274*, *miR-219*, *miR-276a*, *miR-33*, *miR-280*, *miR-281a*, *miR-282*, *miR-284*, *miR-263a*, *miR-289*, *miR-287*, *miR-288*). We added these 12 to the first set and obtained our final dataset. We did not exclude from our dataset the roughly 25% of miRNA genes which were detected in adult animals or testes only, reasoning that the expression assays used are certainly not perfectly sensitive, and also reasoning that we can always backtrack our results.

### *Set of genes important for fly body patterning*

Our set comprises all well known key early genes (*nanos*, *oskar*, *vasa*, *tudor*, *Pumilio*, *Staufen*, *Fat facets*), *gap* (*hunchback*, *bicoid*, *tailless*, *caudal*, *Kruppel*, *giant*, *knirps*, *sloppy paired 1*, *sloppy paired 2*, *buttonhead*, *collier*, *crocodile*, *empty spiracles*, *huckebein*, *orthodenticle*, *cap'n'collar*), and pair-rule genes (*eve*, *hairy*, *ftz*, *runt*, *odd-paired*, *paired*, *Tenascin major*, *odd-skipped*).

### Extraction of 3' UTR sequences in *D. melanogaster* and *D. pseudoobscura*

The 3' UTRs for *D. melanogaster* were extracted from the BDGP genome annotation release 3.1 at [www.fruitfly.org/sequence/download.html](http://www.fruitfly.org/sequence/download.html). The *crocodile* gene from our dataset was the only gene which did not have a 3' UTR of at least 50 base pairs length. In almost all cases where a gene had multiple transcripts, the corresponding 3' UTR sequences were still the same. However, in one case (for the gene *collier*), this was not true, and we chose the transcript CG10197-RB which mapped to the experimentally known cDNA BcDNA:RE03728 of this gene. We note that for roughly 50% of the genes in our dataset, the 3' UTR annotations from release 3.1 are directly supported by the drosophila cDNA library. To define the homologous *D. pseudoobscura* 3' UTR sequences we used the Berkeley genome pipeline (Bray et al., 2003; Couronne et al., 2003) website ([pipeline.lbl.gov/pseudo/](http://pipeline.lbl.gov/pseudo/)) which presents a genomic alignment of the two species. We looked up the corresponding alignments for each *melanogaster* 3' UTR region and extracted the *pseudoobscura* sequence from the alignment with the highest percentage identity. We checked that in each case the coding region of the gene was in the same alignment. The only genes for which we found not enough homology to unambiguously define the *pseudoobscura* 3' UTR were *giant* and *Tenascin major*. These genes were excluded from our dataset. The 3' UTR pairs in our dataset have an average percentage identity of 0.52.

## Results

### *A new algorithm for the computational identification of microRNA target sites recovers known target sites with high specificity*

A careful examination of our set of known miRNA-binding sites revealed in most cases the presence of a GC-rich string of consecutive base pairings with the miRNA. Based on this, we designed a simple scoring scheme that detects this “binding nucleus”. The score for the nucleus is the weighed sum of consecutive base pairs (GC, AU, and GU). We fit these three parameters by maximizing the difference of the mean scores between the training set and random background sequences (“signal”, see Materials and methods) divided by the standard deviation of the background scores (“noise”). We refer to these values as the Z scores (see Fig. 1). The best fit was obtained with the weights  $w_{GC} = 5$ ,  $w_{AU} = 2$ ,  $w_{GU} = 0$ . These values can be scaled by an arbitrary factor. When varying  $w_{GU}$  only slightly, the Z score decreases dramatically, while varying the ratio of  $w_{GC}/w_{AU}$  between 2 and 3 yields comparable Z scores.

These fitted weights give us the best discrimination between the training set and the background. However, a cutoff value of the model score needs to be determined to set

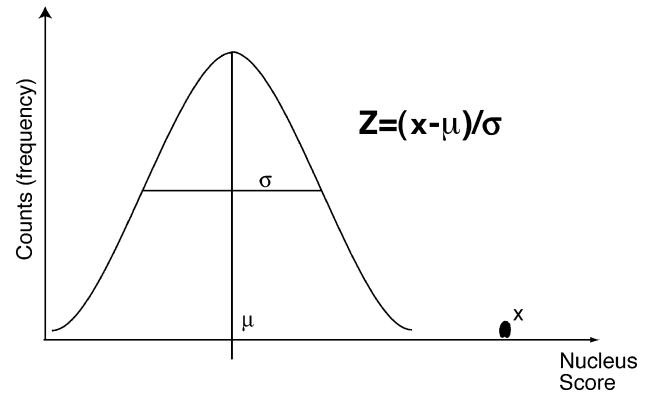


Fig. 1. Pictorial representation of the Z score. The Z score is a comparison of the typical value in the target (training) set with the distribution of scores from the random background. The background distribution is on the left and is parameterized by its mean ( $\mu$ ) and its width (variance). The mean ( $x$ ) of the training set is on the right. The Z score, which represents an approximate signal to noise ratio measurement, is given by  $Z = (x - \mu) / \sigma$ . It indicates how far above the background the target signal is.

the threshold level for target site detection. Naturally, there is a tradeoff between sensitivity and specificity when setting this threshold. For example, for the training set, a threshold value of 25 recovers 84% (21 of 25) of the training data while detecting one false positive per 4000 bases of scanned target sequence. At a higher threshold level of 27, we recover half of the training set and obtain only one false positive per 11,000 bases of target sequence. However, the threshold level chosen for the miRNAs in the training set may not be optimal for other miRNAs. The optimal level may depend on the GC content of the microRNA as well as on other features of sequence composition. Therefore, the threshold score level is set for each miRNA independently by running it over a random sequence and recording the distribution of the scores. From this distribution one can compute  $P$  values for scores. The threshold is then set by cutting off at a desired  $P$  value. Fig. 2 shows the score histogram for one of the training miRNAs (*lin-4*) and demonstrates the specificity of the nucleus score for recovering known target sites.

The size of the nucleus is typically 6–8 bases long and therefore represents less than half the total length of the miRNA. One might expect that one could improve the discrimination between target sites and random sites by incorporating sequence homology between a target site and the miRNA beyond the nucleus. Indeed, *in silico* hybridization of our training target sites to their miRNAs via MFOLD (see Materials and methods) suggests that for most of the RNA/RNA duplexes, a larger fraction of the miRNA is involved in base pairing. Thus, after the binding nucleus was located, a window of 40 bases was extracted from the target sequence and hybridized to the miRNA. The computed binding free energy value is then used to further filter for potential target sites. For example, the combination of nucleus score and free energy at a free energy cutoff of  $-17.4$  kcal/mol further reduced the number of false pos-

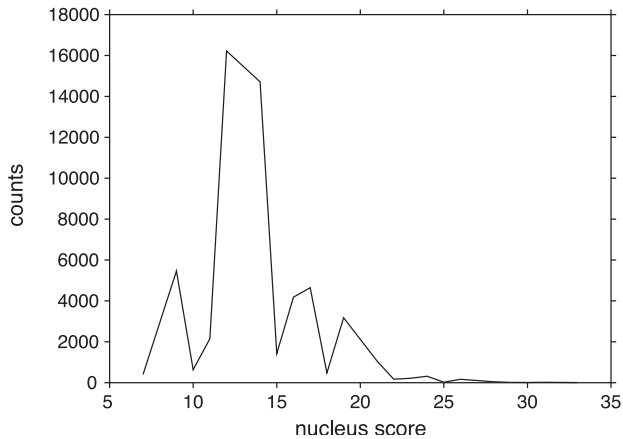


Fig. 2. Nucleus score histogram for the *C. elegans* miRNA *lin-4*. A search window of 30 bases was shifted in steps of 10 over a random sequence of length 1,000,000 bases. At each position, the nucleus score was recorded. A score threshold of 25 (27) will recover 84% (50%) of the known *lin-4* target sites in our training set, but is only rarely exceeded by scores obtained from the random sequence. Thus, the nucleus score recovers with high specificity the known targets.

itives by roughly 10% when detecting half of the known target sites. A few RNA/RNA duplexes in the training set appear to have exceptionally low free energies (lower than roughly  $-27$  kcal/mol). Thus, the free energy can also be used to flag outstanding candidates. However, we note that the main contribution to the specificity of our algorithm stems from the nucleus score. We also note that we tried a great variety of different alignment procedures and screened the parameter space for each one to increase the specificity of the algorithm. None of these approaches outperformed the nucleus score or could efficiently replace MFOLD as a postprocessing step after nucleus scoring.

*The nucleus model recovers known fly bantam targets, and a functionally relevant base in lin-4*

As a test of our nucleus score, we searched the 4017-nucleotide-long *D. melanogaster hid* transcript (*head involution defective*, CG5123-RA, <http://rail.bio.indiana.edu:7084/>) for target sites for the microRNA *bantam* (Brennecke et al., 2003). In Brennecke et al. (2003), five target sites had been verified experimentally. Our nucleus score detected four of them while predicting no other sites. As an additional test, we mutated in silico the cytosine residue of *lin-4* which is essential for posttranscriptional regulation of *lin-14* (Ha et al., 1996). All *lin-14* target sites scored very poorly for this mutation of *lin-4*.

*A simple model for the mechanism of miRNA target recognition*

The ratios of our optimal weights for the nucleus score (which is just the sum over these weights) turn out to correspond well to the experimentally known RNA/RNA

base pairing energy ratios. Thus, our nucleus can be interpreted as a kinetic component of target site recognition: the miRNA needs to be presented with sequence that allows for sufficiently many energetically favorable and consecutive base pairings to rapidly zip up and thereby overcome thermal diffusion.

The second phase of our algorithm models the thermodynamic annealing of the entire miRNA to the target. According to our results, the free energy of the target site/miRNA duplex needs to be lower than roughly half of the free energy of a target site with perfect complementarity to the miRNA. We had found that most of the ability of our algorithm to discriminate target sites from random sites comes from the nucleus. Thus, according to our model, most of the target

Table 1

Putative targets of miRNAs within the set of patterning genes (see Material and methods)

Gene	miRNA	Free eng. position
kn	mir-312	-21.7, 107
kn	mir-313	-22.3, 106
kn	mir-92b	-17, 28
kn	mir-2a-2:mir-2a-1	-18.8, 1078
opa	mir-8	-23.7, 139
oc	mir-317	-23.5, 171 -17.8, 199 -17.8, 205
oc	mir-133	-18.6, 172
btd	mir-7	-18.3, 455
tll	mir-6-1:mir-6-2:mir-6-3	-21.3, 61
tll	miR-219	-27.4, 86
slp1	mir-79	-16.1, 36
slp1	mir-8	-19, 144
cnc	mir-315	-18.5, 983
cnc	mir-279	-18.1, 989 -18.1, 991
run	miR-287	-20,132 -19.5, 334 -18.4, 438
ftz	mir-318	-21.5, 272
ftz	mir-309	-23.4, 271
ftz	mir-263b	-19, 272
ftz	mir275	-23.2, 263
ftz	mir-3	-30.8, 173 -25.8, 272
ems	mir-312	-20, 565
ems	mir-133	-18, 546
ems	miR-263a	-20.8, 422
vas	mir-P323-1:mir-P323-2	-18.3, 668
vas	mir275	-23.8, 637
odd	mir-318	-20.7, 182
odd	mir-263b	-18.7, 182
odd	mir-309	-18.3, 181
odd	mir-5	-22, 673
odd	mir-8	-19.7, 22
odd	mir-3	-20.7, 182
kni	miR-284	-27.8, 144
nos	mir-124	-26.5, 174
stau	miR-280	-16.4, 373
stau	mir305	-29.4, 589
h	miR-289	-22.9, 102
h	let-7	-23.2, 381
h	mir-7	-30.6, 460 -30.6, 461
hkb	let-7	-22.4, 157

The free energy of the predicted RNA/RNA duplexes is given (in kcal/mol) as well as the position of the nucleus in the mRNA (in nucleotides downstream of the stop codon).

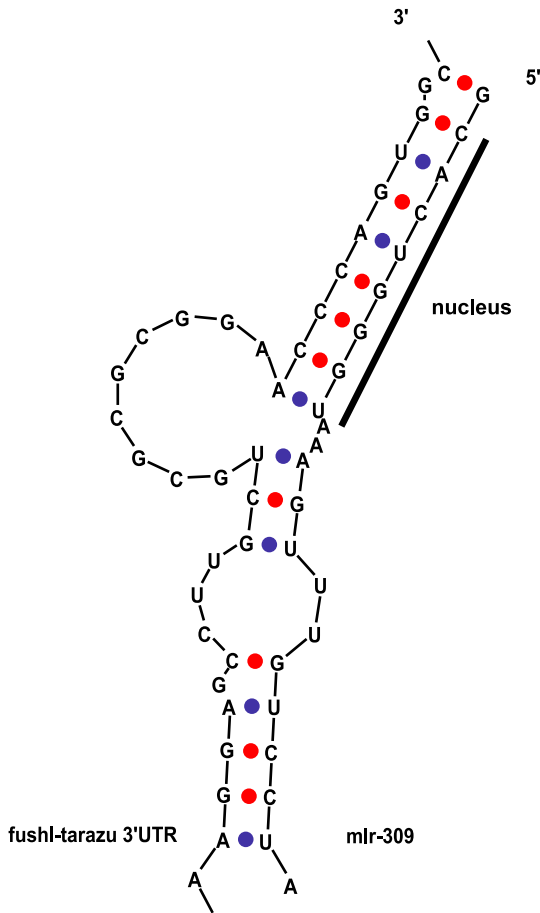


Fig. 3. Predicted targeting of the *D. melanogaster* gene *fushi-tarazu* by *mir-309*. Shown is the mRNA/miRNA duplex as predicted by MFOLD. The free energy is  $-23.4$  kcal/mol, the nucleus has a score of 31 ( $P$  value 0.0001) and is located at the 5' end of the miRNA and 271 bases downstream of the stop codon. The *fushi-tarazu* ortholog in *pseudoobscura* also has a predicted target site for *mir-309*. All nuclei are found close to the 5' end of the miRNA. GC base pairings are marked in red, AU and GU in blue.

recognition seems to take place during the kinetic phase of miRNA to target binding. The model can also explain the observation (Lai, 2002) that some fly miRNA sequences have substrings which are complementary to known 3' UTR sequence motifs that mediate translational repression. However, we remark that the nucleus may not necessarily appear as consecutive base pairs in the predicted secondary structure of the mRNA/microRNA duplex.

#### Searching for new miRNA targets in fly

We applied our algorithm to a set of 74 *D. melanogaster* miRNA genes which have been recently identified (see Materials and methods). The efficiency of the algorithm would allow a genomewide search for targets. However, searching genomewide for targets of a large set of often differentially expressed miRNAs is likely to produce results that are difficult to interpret. Therefore, we decided to focus on a set of 31 well-characterized developmental genes, the body patterning genes (Materials and methods), which are

central to a large regulatory network during development. We reasoned that these genes (many of which are key regulatory genes throughout development) are likely to be targets of certain miRNAs. To further reduce the number of false positives, we limited our search to the 3' UTRs of the genes in our dataset because all known miRNA target sites reside in 3' UTRs. Finally, we filtered all predictions for sites which are, for each *D. melanogaster* 3' UTR, also at least present once in the orthologous *D. pseudoobscura* 3' UTR, reasoning that these sites are more likely to be functional. In our cross-species analysis, we did not make the assumption that target sites reside in a conserved chunk of RNA or that the order of multiple sites in a 3' UTR is the same in both species because we know very little about the evolutionary mechanisms behind 3' UTR sequence evolution. Setting the nucleus score  $P$  value and the RNA/RNA duplex minimal free energy such that we recover 84% of the known targets in our dataset (see above), we found 39 high scoring *melanogaster* putative target sites (see Table 1)

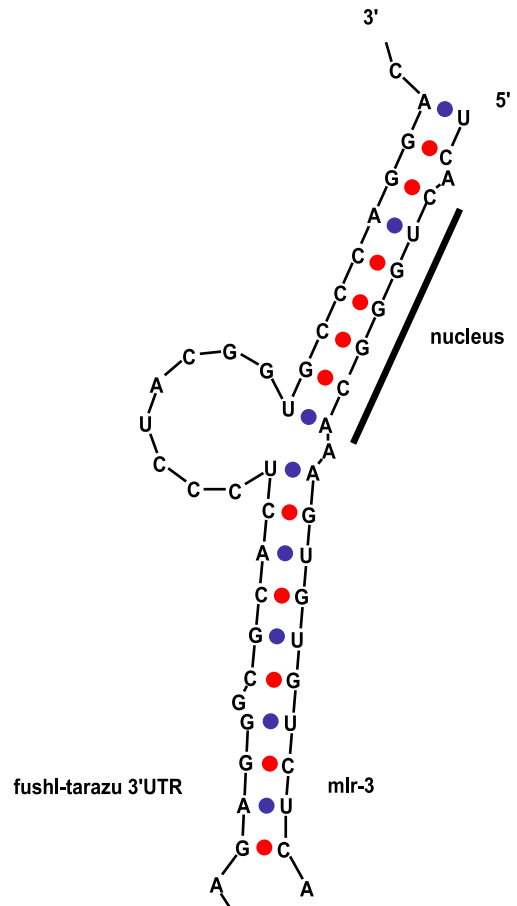


Fig. 4. Predicted targeting of the *D. melanogaster* gene *fushi-tarazu* by *mir-3*. Shown is the mRNA/miRNA duplex as predicted by MFOLD. The free energy is  $-30.8$  kcal/mol, the nucleus has a score of 28 ( $P$  value 0.0001) and is located at the 5' end of the miRNA and 173 bases downstream of the stop codon. Another putative target site for *mir-3* is located 99 bases further downstream. The *fushi-tarazu* ortholog in *pseudoobscura* also has a predicted target site for *mir-3*. All nuclei are found close to the 5' end of the miRNA. GC base pairings are marked in red, AU and GU in blue.

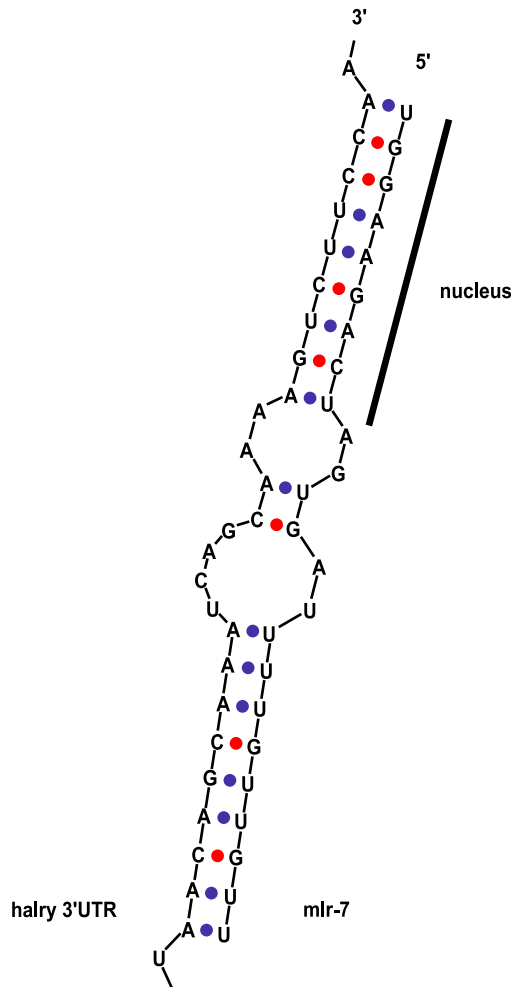


Fig. 5. Predicted targeting of the *D. melanogaster* gene *hairy* by *mir-7*. Shown is the mRNA/miRNA duplex as predicted by MFOLD. The free energy is  $-30.6$  kcal/mol, the nucleus has a score of 30 ( $P$  value 0.0001) and is located at the 5' end of the miRNA. The target site is 438 bases downstream of the stop codon. The *hairy* ortholog in *pseudoobscura* also has a predicted target site for *mir-7*. All nuclei are found close to the 5' end of the miRNA. GC base pairings are marked in red, AU and GU in blue.

which were also present in each case in the orthologous UTR in *pseudoobscura*. Figs. 3–5 present the predicted secondary structures for some of these hits and the position of each nucleus. Detailed analysis of the significance and validation of these data should be accompanied by experiments and is not in the scope of this paper. We will discuss one of the most interesting cases.

The miRNA genes *mir-309*, *mir-318*, *mir-263b*, and *mir-3* all hit the pair-rule genes *fushi-tarazu* and *odd-skipped* and nothing else. Conversely, *fushi-tarazu* does not appear to be targeted by any other miRNAs from our dataset, only *odd-skipped* has additional target sites for *mir-5* and *mir-8* which in turn do not hit any other gene. The position of the nucleus relative to the miRNA is almost perfectly constant for each miRNA across all its hits (e.g., all *mir-309* nuclei are at the 5' end of the miRNA at position 2, all *mir-3* nuclei are at the 5' end of the miRNA at position 1–

4), indicating that the same cis-regulatory motif may be used to coordinate the action of an miRNA across different genes. Again, this observation is consistent with Lai (2002), where it was shown that certain miRNAs are complementary to 3' UTR sequence motifs that mediate negative posttranscriptional regulation.

## Discussion

We found that key developmental genes in fly such as the pair-rule genes *fushi-tarazu*, *odd-skipped*, and *hairy* are possibly targeted by miRNAs (*mir-309*, *mir-318*, *mir-263b*, *mir-3*, and *mir-7*). However, ultimately the function of miRNAs has to be elucidated in the context of their own expression. Some of the above miRNA genes (*mir-3*, *mir-309*, *mir-7*) are indeed known to be expressed during fly development (Aravin et al., 2003). Furthermore, because it seems possible that miRNA genes are transcriptionally regulated similarly to most protein-coding genes (Johnson et al., 2003), we have computationally searched the fly genomes for enhancers near the miRNA gene loci. More precisely, we searched the neighborhood of miRNA gene loci for clusters of binding sites for body-patterning transcription factors using an existing algorithm (Mallela et al., 2003; Rajewsky et al., 2002). We found high scoring clusters very close to some miRNA genes (for example *mir-263b*, Fig. 6) and will test some of these predictions in the future. Hopefully, we will thus understand more about how transcriptional and translational gene regulations are intertwined.

Our algorithm for miRNA target site detection can almost certainly be improved. Because the algorithm is based on experimental knowledge for only two miRNA genes, it seems clear that as new targets for other miRNA genes will be discovered, our understanding and modeling

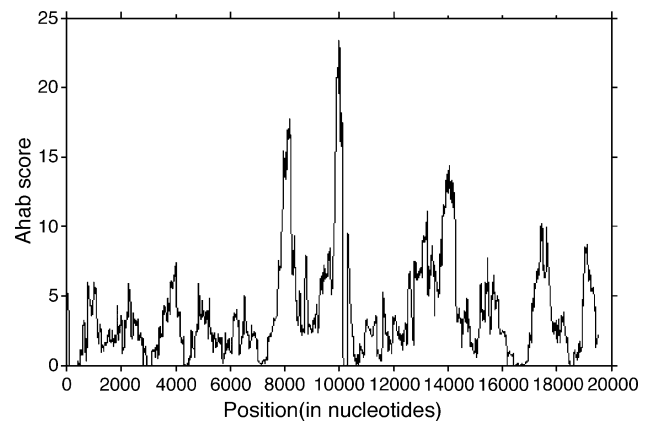


Fig. 6. The *D. melanogaster mir-263b* locus was searched for clusters of binding sites for the body-patterning transcription factors *kruppel*, *caudal*, *bicoid*, *hunchback*, *tailless*, *torRE*, *bicoid* following Rajewsky et al. (2002). We used the Ahab webserver (Mallela et al., 2003). The score for finding a cluster is shown as a function of position in the locus (in nucleotides). Two peaks in the score bracket the position of the miRNA gene.

of the target recognition process will improve and reduce the number of false positives. Furthermore, based on the observation that most genes which are targeted by miRNAs appear to have multiple, co-clustered binding sites for multiple miRNAs in their mRNA and that miRNA genes are thus likely to act combinatorially on target genes (see also Doench et al., 2003), the most substantial improvement could perhaps be made by incorporating searches for clusters of binding sites into the algorithm. Information about expression profiles of miRNA genes will then help to filter for meaningful combinations of miRNA binding sites. Key to further improvements may be to understand more about the evolution of miRNA binding sites and thus to improve cross-species analysis and our understanding how gene regulatory networks evolve.

We have demonstrated that our algorithm can detect miRNA target sites with high specificity, that it leads to a simple model for the mechanisms behind miRNA target site recognition, and that it can be applied to existing data to make testable predictions about miRNA function. Thus, we believe that it will help shed more light on the unfolding, exciting universe of miRNA genes.

## Acknowledgments

We are indebted to Tom Tuschl (Rockefeller University) who shared his unpublished miRNA data with us before publication. We thank Steve Small, Frank Slack, Ralf Bundschuh, and Mihaela Zavolan for stimulating discussions. We also thank Michael Zuker for help with MFOLD. The source code for our algorithm will be available upon request on the authors. While writing this manuscript, we were informed about a similar computational approach by Stephen Cohen's group (EMBL, Heidelberg) and another paper on a related topic by A.J. Enright, B. John, U. Gual, T. Tuschl, C. Sander, and D. Marks which is in press (*Genome Biol.* 2003 (4), 8).

## References

- Ambros, V., 2001. microRNAs: tiny regulators with great potential. *Cell* 107 (7), 823–826.
- Ambros, V., 2003. MicroRNA pathways in flies and worms: growth, death, fat, stress, and timing. *Cell* 113 (6), 673–676.
- Ambros, V., Lee, R.C., Lavanway, A., Williams, P.T., Jewell, D., 2003. MicroRNAs and other tiny endogenous RNAs in *C. elegans*. *Curr. Biol.* 13 (10), 807–818.
- Aravin, A.A., Lagos-Quintana, M., Yalcin, A., Zavolan, M., Marks, D., Snyder, B., Gaasterland, T., Meyer, J., Tuschl, T., 2003. The small RNA profile during *Drosophila melanogaster* development. *Dev. Cell* 5 (2), 337–350.
- Banerjee, D., Slack, F., 2002. Control of developmental timing by small temporal RNAs: a paradigm for RNA-mediated regulation of gene expression. *BioEssays* 24 (2), 119–129.
- Bray, N., Dubchak, I., Pachter, L., 2003. Avid: a global alignment program. *Genome Res.* 13, 97.
- Brennecke, J., Hipfner, D.R., Stark, A., Russell, R.B., Cohen, S.M., 2003. Bantam encodes a developmentally regulated microRNA that controls cell proliferation and regulates the proapoptotic gene *hid* in *Drosophila*. *Cell* 113 (1), 25–36.
- Carrington, J.C., Ambros, V., 2003. Role of microRNAs in plant and animal development. *Science* 301 (5631), 336–338.
- Couronne, O., Poliakov, A., Bray, N., Ishkhanov, T., Ryaboy, D., Rubin, E., Pachter, L., Dubchak, I., 2003. Strategies and tools for whole-genome alignments. *Genome Res.* 13 (1), 73–80.
- Doench, J.G., Petersen, C.P., Sharp, P.A., 2003. siRNAs can function as miRNAs. *Genes Dev.* 17 (4), 438–442.
- Ha, I., Wightman, B., Ruvkun, G., 1996. A bulged lin-4/lin-14 rna duplex is sufficient for *Caenorhabditis elegans* lin-14 temporal gradient formation. *Genes Dev.* 10 (23), 3041–3050.
- Houbaviy, H.B., Murray, M.F., Sharp, P.A., 2003. Embryonic stem cell-specific MicroRNAs. *Dev. Cell* 5 (2), 351–358.
- Johnson, S.M., Lin, S.Y., Slack, F.J., 2003. The time of appearance of the *C. elegans* let-7 microRNA is transcriptionally controlled utilizing a temporal regulatory element in its promoter. *Dev. Biol.* 259 (2), 364–379.
- Lagos-Quintana, M., Rauhut, R., Lendeckel, W., Tuschl, T., 2001. Identification of novel genes coding for small expressed RNAs. *Science* 294 (5543), 853–858.
- Lagos-Quintana, M., Rauhut, R., Yalcin, A., Meyer, J., Lendeckel, W., Tuschl, T., 2002. Identification of tissue-specific microRNAs from mouse. *Curr. Biol.* 12 (9), 735–739.
- Lai, E.C., 2002. Micro RNAs are complementary to 3' UTR sequence motifs that mediate negative post-transcriptional regulation. *Nat. Genet.* 30 (4), 363–364.
- Lai, E.C., Tomancak, P., Williams, R.W., Rubin, G.M., 2003. Computational identification of drosophila microRNA genes. *Genome Biol.* 4 (7), R42.
- Lau, N.C., Lim, L.P., Weinstein, E.G., Bartel, D.P., 2001. An abundant class of tiny RNAs with probable regulatory roles in *Caenorhabditis elegans*. *Science* 294 (5543), 858–862.
- Lee, R.C., Ambros, V., 2001. An extensive class of small RNAs in *Caenorhabditis elegans*. *Science* 294 (5543), 862–864.
- Lim, L.P., Glasner, M.E., Yekta, S., Burge, C.B., Bartel, D.P., 2003a. Vertebrate microRNA genes. *Science* 299 (5612), 1540.
- Lim, L.P., Lau, N.C., Weinstein, E.G., Abdelhakim, A., Yekta, S., Rhoades, M.W., Burge, C.B., Bartel, D.P., 2003b. The microRNAs of *Caenorhabditis elegans*. *Genes Dev.* 17 (8), 991–1008.
- Lin, S.-Y., Johnson, S.M., Abraham, M., Vella, M.C., Pasquinelli, A., Gamberi, C., Gottlieb, E., Slack, F.J., 2003. The *C. elegans* hunchback homolog, hbl-1, controls temporal patterning and is a probable microRNA target. *Dev. Cell* 4 (5), 639–650.
- Mallela, J., Kacmarczyk, T., Bonavia, A., Rajewsky, N., 2003. The Ahab Webserver. <http://gaspard.bio.nyu.edu/Ahab.html>, unpublished.
- Moss, E.G., 2002. MicroRNAs: hidden in the genome. *Curr. Biol.* 12 (4), R138–R140.
- Moss, E.G., Poethig, R.S., 2002. MicroRNAs: something new under the sun. *Curr. Biol.* 12 (20), R688–R690.
- Rajewsky, N., Vergassola, M., Gaul, U., Siggia, E.D., 2002. Computational detection of genomic cis-regulatory modules applied to body patterning in the early drosophila embryo. *BMC Bioinformatics* 3 (1), 30.
- Rhoades, M.W., Reinhart, B.J., Lim, L.P., Burge, C.B., Bartel, B., Bartel, D.P., 2002. Prediction of plant microRNA targets. *Cell* 110 (4), 513–520.
- Xu, P., Vernooy, S.Y., Guo, M., Hay, B.A., 2003. The drosophila microRNA mir-14 suppresses cell death and is required for normal fat metabolism. *Curr. Biol.* 13 (9), 790–795.
- Zuker, M., 2003. Mfold web server for nucleic acid folding and hybridization prediction. *Nucleic Acids Res.* 31 (13), 3406–3415.